Adaptive evolution of drug targets in producer and non-producer organisms

Hansen, Bjarne Gram; Sun, Xin E.; Genee, Hans Jasper; Kaas, Christian Schrøder; Hoof, Jakob Blæsbjerg; Frisvad, Jens Christian; Hedstrom, Lizbeth

Published in:
Biochemical Journal

Link to article, DOI:
10.1042/BJ20111278

Publication date:
2012

Document Version
Publisher's PDF, also known as Version of record

BJ www.biochemj.org

BJ Structure

Biochem. J. (2012) **441**, 219–226 (Printed in Great Britain) doi:10.1042/BJ20111278

online data

Adaptive evolution of drug targets in producer and non-producer organisms

Bjarne G. HANSEN*[1], Xin E. SUN†[2], Hans J. GENEE*, Christian S. KAAS*, Jakob B. NIELSEN*, Uffe H. MORTENSEN*, Jens C. FRISVAD* and Lizbeth HEDSTROM‡[3]

*Technical University of Denmark, Department of Systems Biology, Center for Microbial Biotechnology, 2800 Kgs Lyngby, Denmark, †Graduate Program in Biochemistry, Brandeis University, 415 South Street, Waltham, MA 02454, U.S.A., and ‡Departments of Biology and Chemistry, Brandeis University, 415 South Street, Waltham, MA 02454, U.S.A.

MPA (mycophenolic acid) is an immunosuppressive drug produced by several fungi in *Penicillium* subgenus *Penicillium*. This toxic metabolite is an inhibitor of IMPDH (IMP dehydrogenase). The MPA-biosynthetic cluster of *Penicillium brevicompactum* contains a gene encoding a B-type IMPDH, IMPDH-B, which confers MPA resistance. Surprisingly, all members of the subgenus *Penicillium* contain genes encoding IMPDHs of both the A and B types, regardless of their ability to produce MPA. Duplication of the IMPDH gene occurred before and independently of the acquisition of the MPA-biosynthetic cluster. Both *P. brevicompactum* IMPDHs are MPA-resistant, whereas the IMPDHs from a non-producer are MPA-sensitive. Resistance comes with a catalytic cost: whereas *P. brevicompactum* IMPDH-B is >1000-fold more resistant to MPA than a typical eukaryotic IMPDH, its k_{cat}/K_m value is 0.5 % of 'normal'. Curiously, IMPDH-B of *Penicillium chrysogenum*, which does not produce MPA, is also a very poor enzyme. The MPA-binding site is completely conserved among sensitive and resistant IMPDHs. Mutational analysis shows that the C-terminal segment is a major structural determinant of resistance. These observations suggest that the duplication of the IMPDH gene in the subgenus *Penicillium* was permissive for MPA production and that MPA production created a selective pressure on IMPDH evolution. Perhaps MPA production rescued IMPDH-B from deleterious genetic drift.

Key words: drug resistance, gene duplication, IMP dehydrogenase (IMPDH), mycophenolic acid, neofunctionalization, *Penicillium*.

INTRODUCTION

Filamentous fungi produce a vast arsenal of toxic natural products that require the presence of corresponding defence mechanisms to avoid self-intoxication. The importance of these defence mechanisms is demonstrated by the presence of resistance genes within biosynthetic gene clusters, yet how production and resistance co-evolved is poorly understood. Insights into the inhibition of enzymes involved in self-resistance provide an intriguing strategy for the development of antifungal agents. Furthermore, the elucidation of the defence mechanisms is required for the design of heterologous cell factories producing bioactive compounds.

Self-resistance can involve expression of a target protein that is impervious to the toxic natural product, which suggests that resistance originates from a gene-duplication event. The biosynthetic cluster of the immunosuppressive drug MPA (mycophenolic acid) offers an intriguing example of this phenomenon. MPA is a well-characterized inhibitor of IMPDH (IMP dehydrogenase) [1], and the *Penicillium brevicompactum* MPA-biosynthetic cluster contains a second type of IMPDH gene that confers MPA resistance (IMPDH-B/*mpaF*) [2,3]. Curiously, both MPA producers and non-producers in *Penicillium* subgenus *Penicillium* contain two IMPDH genes encoding IMPDH-A and IMPDH-B [3]. Phylogenetic analysis suggests that the gene-duplication event occurred before or simultaneous with the radiation of *Penicillium* subgenus *Penicillium* [2,3]. How this gene-duplication event influenced the acquisition of MPA biosynthesis is not understood.

In the present study, we investigated the relationship between MPA production, MPA resistance and the properties of IMPDH-A and IMPDH-B. Whereas IMPDH-B from the producer organism *P. brevicompactum* is extraordinarily resistant to MPA, IMPDH-B from the non-producer *Penicillium chrysogenum* displays typical sensitivity. Both IMPDH-Bs are very poor enzymes, but *P. chrysogenum* IMPDH-B is almost non-functional. These observations suggest that acquisition of the MPA biosynthetic cluster may have rescued IMPDH-B from deleterious genetic drift.

EXPERIMENTAL

Fungal strains

P. brevicompactum IBT23078, *P. chrysogenum* IBT5857, *Aspergillus nidulans* IBT27263, and the 11 strains listed in Supplementary Table S1 (at http://www.BiochemJ.org/bj/441/bj4410219add.htm), were grown on CYA (Czapek yeast extract agar) at 25 °C [4].

MPA treatment of fungi

Spores from *P. brevicompactum* IBT23078, *P. chrysogenum* IBT5857 and *A. nidulans* IBT27263 were harvested and suspended in sterile water. Then, 10 μl of serial 10-fold spore dilutions were spotted on to CYA plates with or without 200 μg/ml MPA. All plates contained 0.8 % methanol. Stock solution (25 mg/ml MPA in methanol) and MPA plates were made briefly

Abbreviations used: CYA, Czapek yeast extract agar; dPCR, degenerate PCR; DTT, dithiothreitol; gDNA, genomic DNA; IMPDH, IMP dehydrogenase; *An*ImdA, IMPDH-A from *Aspergillus nidulans*; *Pb*IMPDH-A, IMPDH-A from *Penicillium brevicompactum*; *Pb*IMPDH-B, IMPDH-B from *P. brevicompactum*; *Pc*IMPDH-A, IMPDH-A from *Penicillium chrysogenum*; *Pc*IMPDH-B, IMPDH-B from *P. chrysogenum*; IPTG, isopropyl β-D-thiogalactopyranoside; LB, Luria–Bertani; MPA, mycophenolic acid.

[1] Present address: Novozymes A/S, Krogshoejvej 36, 2880 Bagsvaerd, Denmark.
[2] Present address: Department of Chemistry, Boston University, 590 Commonwealth Avenue, Boston, MA 02215-252, U.S.A.
[3] To whom correspondence should be addressed (email hedstrom@brandeis.edu).

before the spores were spotted on to the plates in order to avoid MPA degradation. MPA was acquired from Sigma.

RNA purification and cDNA synthesis

Spores from *P. brevicompactum* IBT23078 were harvested and used to inoculate 200 ml of YES (yeast extract sucrose) medium in 300 ml shake flasks without baffles [4]. *P. brevicompactum* was grown at 25 °C and 150 rev./min shaking. After 48 h, the mycelium was harvested and RNA was purified using the Fungal RNA purification Miniprep Kit (E.Z.N.A.) and cDNA was synthesized from the RNA using Finnzymes Phusion™ RT (reverse transcription)–PCR kit following the instructions of the two manufacturers.

Plasmid construction

Constructs for expression of His_6-tagged IMPDHs in *Escherichia coli* were created by inserting the IMPDH coding sequences into pET28a that had been converted into a USER-compatible vector (see Supplementary Figure S1 at http://www.BiochemJ.org/bj/441/bj4410219add.htm). pET28U was created by PCR-amplifying pET28 with the primers BGHA527/BGHA528 followed by DpnI treatment to remove the PCR template (see Supplementary Figure S1). The *P. brevicompactum* IMPDH-B (*Pb*IMPDH-B) gene was amplified from cDNA from *P. brevicompactum*. Genes encoding *A. nidulans* IMPDH-A (*An*ImdA), *P. brevicompactum* IMPDH-A (*Pb*IMPDH-A), *P. chrysogenum* IMPDH-A (*Pc*IMPDH-A) and *P. chrysogenum* IMPDH-B (*Pc*IMPDH-B) were obtained from gDNA (genomic DNA). In all cases, the three exons of each gene were individually PCR-amplified and purified and subsequently USER-fused using a method described previously [5,6].

The expression constructs for chimaeric and mutated IMPDHs were created by fusing the two parts of the IMPDHs using the USER fusion method to introduce the mutation in the primer tail [6]. Chimaeric IMPDH of *Pb*IMPDH-B (N-terminus) and *Pb*IMPDH-A (C-terminus) was created by USER-fusing two *P. brevicompactum* IMPDH-B and IMPDH-A fragments, which were PCR-amplified with primer pairs BGHA529/BGHA667 and BGHA668/BGHA540 respectively, into pET28U as described above. Similarly, chimaeric IMPDH of *Pb*IMPDH-A (N-terminus) and *Pb*IMPDH-B (C-terminus) was created by amplifying *Pb*IMPDH-A and *Pb*IMPDH-B fragments with primer pairs BGHA539/BGHA669 and BGHA670/BGHA530 respectively, followed by USER-fusing into pET28U. Using gDNA from the proper source, the Y411F (Chinese-hamster ovary IMPDH2 numbering) mutation was introduced into *A. nidulans* IMPDH-A and into *P. brevicompactum* IMPDH-A and IMPDH-B by amplifying and fusing two IMPDH fragments with primer pairs BGHA545/BGHA359 and BGHA546/BGHA358; BGHA539/BGHA455 and BGHA540/BGHA454; and BGHA529/BGHA361 and BGHA530/BGHA360 respectively. For details of primers, see Supplementary Tables S2 and S3 (at http://www.BiochemJ.org/bj/441/bj4410219add.htm). The PfuX7 polymerase was used for PCR amplification in all cases [7].

Cladistic analysis

Alignment of DNA coding regions and protein were performed with ClustalW implemented in the CLC DNA Workbench 6 program (CLC bio) using the following parameters: gap open cost = 6.0; gap extension cost = 1.0; and end gap cost = free. A cladogram was constructed with the same software using the neighbour-joining method and 1000 bootstrap replicates [33]. The DNA sequence of IMPDH and β-tubulin from selected fungi were either generated by dPCR (degenerate PCR) (see Supplementary Table S1) or retrieved from the NCBI: *A. nidulans* β-tubulin (GenBank® accession number XM_653694) and IMPDH-A DNA sequence [GenBank® accession number BN001302 (ANIA_10476)]; *Coccidioides immitis* β-tubulin (GenBank® accession number XM_001243031) and IMPDH-A DNA sequence (GenBank® accession number XM_001245054); *Penicillium bialowiezense* IBT21578 β-tubulin (GenBank® accession number JF302653), IMPDH-A DNA sequence (GenBank® accession number JF302658) and IMPDH-B DNA sequence (GenBank® accession number JF302662); *P. brevicompactum* IBT23078 β-tubulin (GenBank® accession number JF302653) and IMPDH-A DNA sequence (GenBank® accession number JF302657); *Penicillium carneum* IBT3472 β-tubulin (GenBank® accession number JF302650), IMPDH-A DNA sequence (GenBank® accession number JF302656) and IMPDH-B DNA sequence (GenBank® accession number JF302660); *P. chrysogenum* IBT5857 β-tubulin (GenBank® accession number XM_002559715), IMPDH-A DNA sequence (GenBank® accession number XM_002562313) and IMPDH-B DNA sequence (GenBank® accession number XM_002559146); *Penicillium paneum* IBT21729 β-tubulin (GenBank® accession number JF302651), IMPDH-A DNA sequence (GenBank® accession number JF302654) and IMPDH-B DNA sequence (GenBank® accession number JF302661); and *Penicillium roqueforti* IBT16406 β-tubulin (GenBank® accession number JF302649), IMPDH-A DNA sequence (GenBank® accession number JF302655) and IMPDH-B DNA sequence (GenBank® accession number JF302659). The MPA gene cluster sequence from *P. brevicompactum* IBT23078, which contains the IMPDH-B gene sequence (*mpaF*) is available from GenBank® under accession number HQ731031. Full-length protein sequences were retrieved from the NCBI: *Candida albicans*: (GenBank® accession number EEQ46038), Chinese-hamster ovary IMPDH2 (GenBank® accession number P12269), *E. coli* (GenBank® accession number ACI80035), human IMPDH type 2 (GenBank® accession number NP_000875), *P. chrysogenum* IMPDH-A gene (GenBank® accession number CAP94756), IMPDH-B (GenBank® accession number CAP91832), yeast IMD2 (GenBank® accession number P38697), IMD3 (GenBank® accession number P50095), and IMD4 (GenBank® accession number P50094).

dPCR

Primers and PCR conditions for amplifying part of the genes encoding IMPDH-A, IMPDH-B and β-tubulin were as described in [3]. Genomic DNA from 11 fungi from the *Penicillium* subgenus *Penicillium* subclade (see Supplementary Table S1) were extracted using the FastDNA® SPIN for Soil Kit (MP Biomedicals). PCR primer pairs BGHA236HC/BGHA246HC or BGHA531/BGHA532 were used to amplify DNA from the gene encoding IMPDH-A. The primer pair BGHA240HC/BGHA241HC was used to amplify DNA from the gene encoding IMPDH-B, and the primer pair BGHA343/BGHA344 was used to amplify β-tubulin.

Expression and purification of His_6-tagged proteins

Plasmids were expressed in a Δ*guaB* derivative of *E. coli* BL21(DE3) [8]. Cells were grown in LB (Luria–Bertani) medium at 30 °C until reaching a D_{600} of 1.0 for *An*ImdA and 1.5 for

all other enzymes, and induced overnight at 16 °C with 0.5 mM IPTG (isopropyl β-D-thiogalactopyranoside) for *An*ImdA and 0.1 mM IPTG for all other enzymes. Cells were harvested by centrifugation at 3000 ***g*** for 20 min and resuspended in buffer (pH 8.0) containing 20 mM sodium phosphate, 500 mM NaCl, 5 mM 2-mercaptoethanol, 5 mM imidazole and Complete™ protease inhibitor cocktail (Roche Diagnostics). Cell lysates were prepared by sonication followed by centrifugation at 40 000 ***g*** for 30 min. All enzymes were purified using a HisTrap affinity column (GE Healthcare) on an ÄKTA Purifier (GE Healthcare) and dialysed into buffer containing 50 mM Tris/HCl, pH 8.0, 100 mM KCl, 1 mM DTT (dithiothreitol) and 10 % glycerol. All enzymes were purified to >90 % purity as determined by SDS/PAGE (12% gels), with the exception of *Pc*IMPDH-B, which was only partially purified to ~45 % purity due to poor expression and stability (see Supplementary Figure S2 at http://www.BiochemJ.org/bj/441/bj4410219add.htm).

Enzyme concentration determination

Enzyme concentration was determined using the Bio-Rad assay according to the manufacturer's instructions using IgG as a standard. The Bio-Rad assay overestimates the IMPDH concentration by a factor of 2.6 [9]. Concentration of active enzyme was determined by MPA titration using an equation for tight binding inhibition (eqn 1):

$$v_i/v_0 = (1 - \{([E] + [I] + IC_{50}) - (\{([E] + [I] + IC_{50})^2\} - 4E \cdot [I])^{0.5}\}/(2[E])) \quad (1)$$

Enzyme assays

Standard IMPDH assay buffer consisted of 50 mM Tris/HCl (pH 8.0), 100 mM KCl, 1 mM DTT, and various concentrations of IMP and NAD^+ (concentrations used for each enzyme are listed in Supplementary Table S4 at http://www.BiochemJ.org/bj/441/bj4410219add.htm. Enzyme activity was measured by monitoring the production of NADH by changes in absorbance increase at 340 nm on a Cary Bio-100 UV–visible spectrophotometer at 25 °C ($\varepsilon_{340} = 6.2\,mM^{-1}\cdot cm^{-1}$). MPA inhibition assays were performed at saturating IMP and half-saturating NAD^+ concentrations to avoid complications arising from NAD^+ substrate inhibition. IMP-independent reduction of NAD^+ was observed in the partially purified preparation of *Pc*IMPDH-B at ~25 % of the rate in the presence of IMP. The rate of this background reaction was subtracted from the rate with IMP for each MPA concentration. Initial velocity data were obtained by fitting to either the Michaelis–Menten equation (eqn 2) or an uncompetitive substrate inhibition equation (eqn 3) using SigmaPlot (Systat Software).

$$v = V_m[S]/(K_m + [S]) \quad (2)$$

$$v = V_m/\{1 + (K_m/[S]) + ([S]/K_{ii})\} \quad (3)$$

Bacterial complementation assays

Cultures were grown overnight in LB medium with 25 μg/ml kanamycin. Then, 5 μl of 1:20 serial dilutions was plated on M9 minimal medium containing 0.5 % casamino acids, 100 μg/ml L-tryptophan, 0.1 % thiamine, 25 μg/ml kanamycin and 66 μM IPTG. Guanosine-supplemented plates contained 50 μg/ml guanosine. MPA plates contained 100 μM MPA. Plates were incubated overnight at 37 °C and then grown at room temperature (25 °C).

Sequences generated in the present study

See Supplementary Table S1 for GenBank® accession numbers.

RESULTS

The presence of IMPDH-B is not linked to MPA biosynthesis

The first gene encoding IMPDH-B was identified in *P. brevicompactum* where it is part of the MPA biosynthetic cluster and confers MPA resistance (*P. brevicompactum* IMPDH-B is also known as *mpaF*) [2]. Of the full genome sequences currently available for filamentous fungi, only *P. chrysogenum* (the sole representative of *Penicillium* subgenus *Penicillium*) contains an IMPDH-B gene. We previously analysed four other fungi in *Penicillium* subgenus *Penicillium* for the presence of IMPDH genes, and all contain both IMPDH-A and IMPDH-B [3]. We have now expanded this search to include 11 additional *Penicillium* strains of the *Penicillium* subgenus. dPCR analysis revealed that all 11 strains contain both genes encoding IMPDH-A and IMPDH-B (see Supplementary Table S1 and Supplementary Figure S3 at http://www.BiochemJ.org/bj/441/bj4410219add.htm), suggesting that the presence of IMPDH-B is widespread in species of *Penicillium* subgenus *Penicillium*, even though many of these strains do not produce MPA [10].

It is possible that these MPA non-producer strains may contain latent or cryptic MPA biosynthetic genes. A previously described example is that although *P. chrysogenum* does not produce viridicatumtoxin, griseofulvin and tryptoquialanine, it does contain sequence regions with high identity with these biosynthetic clusters, which suggests that these gene functions were lost during evolution [11,12]. Likewise, *P. chrysogenum* does not produce MPA. However, in this case, BLAST searches failed to identify any genes with significant sequence identity with the MPA biosynthesis gene cluster in *P. chrysogenum*. These searches did identify an IMPDH-B pseudogene in *P. chrysogenum.* This 260 bp gene fragment has highest identity with IMPDH-B from *P. chrysogenum* (77 %) and 64 % identity with IMPDH-B from *P. brevicompactum*.

We analysed the regions surrounding the MPA biosynthetic cluster in *P. brevicompactum* and used BLAST searches to identify similar genes in *P. chrysogenum.* In this way, adjacent genes that are highly similar and syntenic to genes found in *P. chrysogenum* were identified (Figure 1). Interestingly, the genes flanking one side of the cluster correspond to a locus on contig Pc0022, while the other side of the cluster corresponds to a locus located at another contig, Pc0021. Regions further away from the MPA cluster in *P. brevicompactum* contain additional homologues of *P. chrysogenum* genes, but these genes are located in many different contigs (see Supplementary Table S5 at http://www.BiochemJ.org/bj/441/bj4410219add.htm). *P. chrysogenum* contains small sequence regions with high identity with the flanking region of the MPA cluster. This identity is in the promoter regions and probably represents conserved regulatory regions. Despite a detailed search, we found no sequence similarity to the regions around the *Pc*IMPDH-B and the pseudo IMPDH-B (Pc22g07570) (results not shown). Together, these findings suggest that the MPA cluster has never been present in *P. chrysogenum* and that a high degree of genome shuffling has occurred since the divergence of *P. brevicompactum* and *P. chrysogenum*.

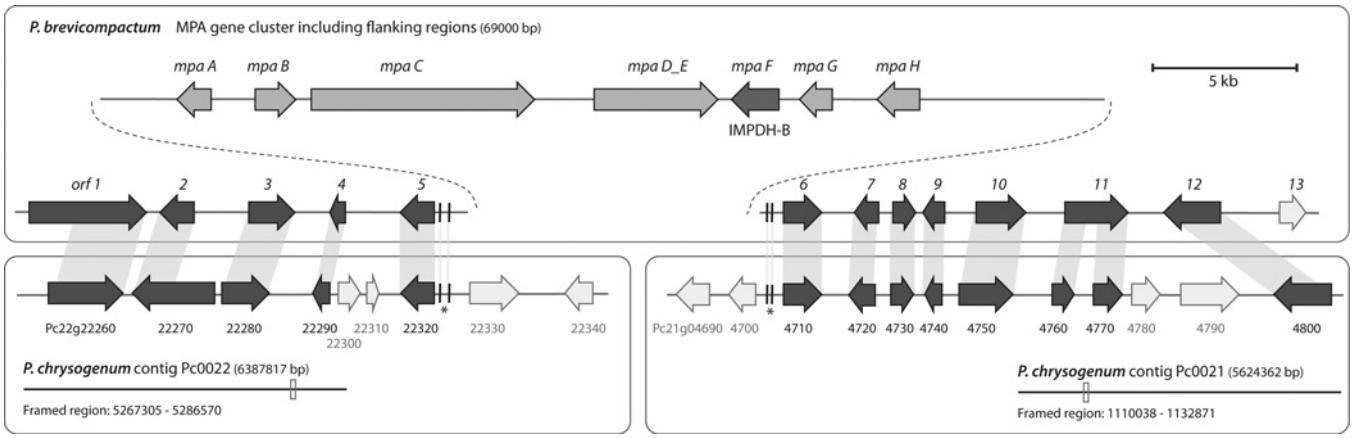

Figure 1 Flanking regions of the MPA-biosynthesis gene cluster

P. brevicompactum and the corresponding syntenic loci on *P. chrysogenum* contigs Pc0022 and Pc0021 are shown. Regions marked with (*) indicate short conserved sequences (length <53 bp, identity >86 %).

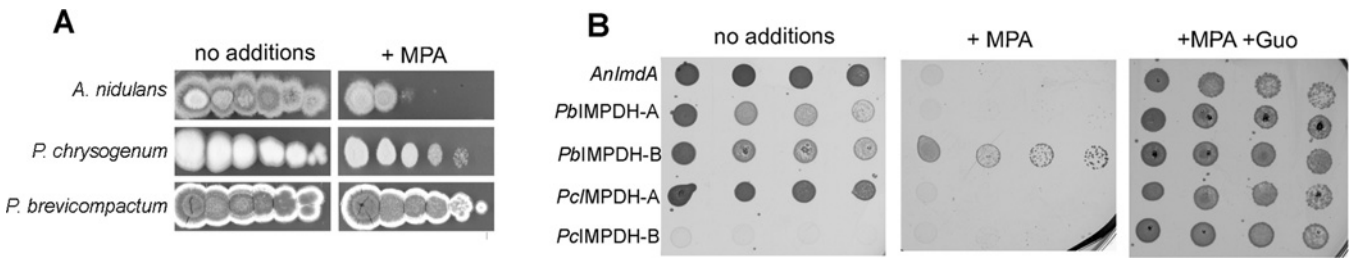

Figure 2 MPA resistance in fungi and bacteria expressing fungal IMPDHs

(**A**) Spot assay to determine sensitivity towards MPA. A 10-fold dilution series of spores from *A. nidulans*, *P. chrysogenum* and *P. brevicompactum* were grown on CYA plates containing no additives or 6.2 μM MPA. The spot with the highest number of spores in each row contains $\sim 10^6$ spores. (**B**) *E. coli* Δ*guaB* was cultured on minimal medium, with no additions or supplemented with 100 μM MPA or 50 μg/ml guanosine (Guo) and 100 μM MPA.

*Pb*IMPDH-B is MPA-resistant, but *Pc*IMPDH-B is MPA-sensitive

The *Pb*IMPDH-B gene confers MPA resistance on *A. nidulans*, suggesting that MPA resistance might be a common feature of all IMPDH-B proteins [3]. Consistent with this hypothesis, *P. chrysogenum* is less sensitive to MPA than *A. nidulans*, although significantly more sensitive than *P. brevicompactum* (Figure 2A). These observations suggest that *P. chrysogenum* IMPDH-B may be semi-resistant to MPA.

To investigate this hypothesis further, IMPDHs from *P. brevicompactum*, *P. chrysogenum* and *A. nidulans* were heterologously expressed as N-terminal His_6-tagged proteins in an *E. coli* Δ*guaB* strain that lacks endogenous IMPDH; these enzymes are denoted *Pb*IMPDH-A, *Pb*IMPDH-B, *Pc*IMPDH-A, *Pc*IMPDH-B and *An*ImdA (Figure 2B). All strains grow on minimal medium in the presence of guanosine (Figure 2B). Bacteria expressing *An*ImdA, *Pb*IMPDH-A, *Pb*IMPDH-B and *Pc*IMPDH-A grow on minimal medium in the absence of guanosine, indicating that active IMPDHs were expressed in all four cases. Only bacteria expressing *Pb*IMPDH-B were resistant to MPA (Figure 2B). *Pc*IMPDH-B failed to grow on minimal medium in the absence of guanosine, suggesting that this protein was not able to complement the *guaB* deletion. This observation suggests that *Pc*IMPDH-B may be non-functional.

All five fungal IMPDHs were isolated to investigate further the molecular basis of MPA resistance. With the exception of *Pc*IMPDH-B, all enzymes were purified to >90 % purity in one step using a nickel-affinity column (see Supplementary Figure S2). *Pc*IMPDH-B was unstable and could only be purified to ∼45 % homogeneity. Western blot analysis using anti-(human IMPDH2) polyclonal antibodies showed that *Pc*IMPDH-B had undergone proteolysis. This degradation could not be prevented by the inclusion of protease inhibitor cocktails during the purification. We performed MPA titrations to determine the concentration of active enzyme in all five protein samples. MPA traps an intermediate in the IMPDH reaction, so that only active enzyme will bind MPA [13]. All of the proteins were ∼100 % active, with the exception of *Pc*IMPDH-B, which was 48 % active, as expected. The oligomeric states of *An*ImdA, *Pb*IMPDH-A and *Pb*IMPDH-B were examined by gel-filtration chromatography. All three enzymes eluted at a molecular mass of approximately 220 kDa, consistent with being tetramers (see Supplementary Figure S3).

*An*ImdA, *Pc*IMPDH-A and *Pc*IMPDH-B are all sensitive to MPA, with values of IC_{50} ranging from 26 to 60 nM (Figure 3 and Table 1). Similar MPA inhibition has been reported for the mammalian and *C. albicans* enzymes [13,14]. These observations indicate that MPA resistance is not a general property of IMPDH-Bs.

MPA is a poor inhibitor of both *Pb*IMPDH-A and *Pb*IMPDH-B (Figure 3 and Table 1). *Pb*IMPDH-A is 10-fold more resistant than IMPDHs from the other filamentous fungi whereas *Pb*IMPDH-B is a remarkable ∼1000-fold more resistant. Thus the ability of *P. brevicompactum* to proliferate while producing MPA can be explained by the intrinsic resistance of its target enzymes. These observations suggest that MPA production creates a selective

Table 1 Characterization of IMPDHs from filamentous fungi

Data were analysed as described in the Experimental section. n.a., not applicable. *Pb*IMPDH-B and *Pc*IMPDH-B did not show NAD^+ substrate inhibition up to 5 mM. The concentrations of IMP and NAD^+ used for IC_{50} determination for each enzyme is included in Supplementary Table S4 at http://www.BiochemJ.org/bj/441/bj4410219add.htm.

Enzyme	IC_{50} (MPA) (μM)	k_{cat} (s^{-1})	K_m (IMP) (μM)	k_{cat}/K_m (IMP) ($M^{-1}\cdot s^{-1}$)	K_m (NAD^+) (μM)	k_{cat}/K_m (NAD) ($M^{-1}\cdot s^{-1}$)	K_{ii} (NAD^+) (mM)
*An*ImdA	0.026 ± 0.002	0.74 ± 0.06	10 ± 1	74000 ± 8000	170 ± 70	4400 ± 100	1.5 ± 0.6
*Pb*IMPDH-A	0.43 ± 0.03	0.70 ± 0.08	130 ± 30	5400 ± 1200	340 ± 90	2100 ± 900	4.7 ± 1.1
*Pb*IMPDH-B	27 ± 9	0.41 ± 0.02	1400 ± 200	300 ± 80	790 ± 140	500 ± 100	n.a.
*Pc*IMPDH-A	0.036 ± 0.004	0.84 ± 0.03	40 ± 6	21000 ± 2000	290 ± 60	2900 ± 300	2.4 ± 0.5
*Pc*IMPDH-B	0.06 ± 0.01	0.0075 ± 0.001	600 ± 300	12 ± 3	640 ± 130	11 ± 6	n.a.

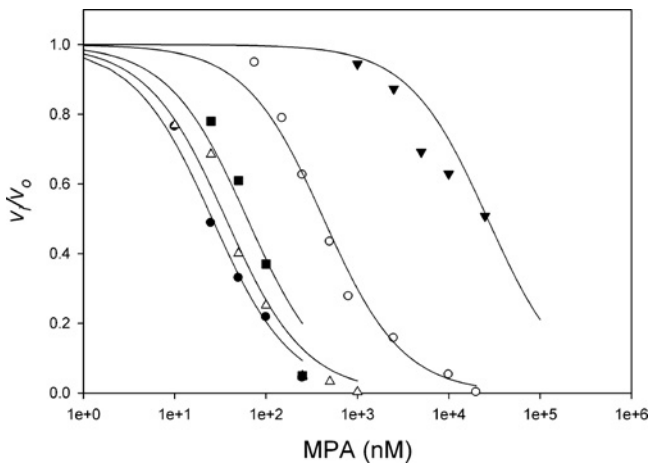

Figure 3 MPA inhibition of fungal IMPDHs

●, *An*ImdA; ○, *Pb*IMPDH-A; ▼, *Pb*IMPDH-B; △, *Pc*IMPDH-A; ■, *Pc*IMPDH-B.

pressure on IMPDH evolution. Curiously, similar IC_{50} values have been reported for Imd2 and Imd3 from *Saccharomyces cerevisiae* ($IC_{50} = 70\ \mu$M and 500 nM for Imd2 and Imd3 respectively [15]). These enzymes are the only other examples of naturally occurring MPA-resistant IMPDHs from eukaryotes. Cladistic analysis indicates that the *S. cerevisiae* IMPDHs arose in a distinct gene-duplication event (Figure 4). Therefore *P. brevicompactum* IMPDH-B is unlikely to share a common ancestry with *S. cerevisiae* Imd2.

IMPDH-Bs are very poor IMPDHs

The reactions of the fungal IMPDHs were characterized to determine how MPA resistance affects enzymatic function. The values of k_{cat} are similar for *An*ImdA, *Pc*IMPDH-A, *Pb*IMPDH-A and *Pb*IMPDH-B, and generally typical for eukaryotic IMPDHs [13] (Table 1). Typical values of K_m (NAD^+) and K_m (IMP) are also observed for *An*ImdA and *Pc*IMPDH-A; the values of K_m for *Pb*IMPDH-A are high, but not unprecedented. In contrast, the value of K_m (IMP) for *Pb*IMPDH-B (1.4 mM) is ~100-fold higher than the highest value reported for any other IMPDH. Like *Pb*IMPDH-B, *Pc*IMPDH-B exhibits an abnormally high value of K_m (IMP). The value of k_{cat} of *Pc*IMPDH-B is more than a factor of 100 less than those of the other fungal IMPDHs. The corresponding values of k_{cat}/K_m are the lowest ever observed for an IMPDH by factors of 1000 (IMP) and 200 (NAD^+) (see [13] for compilation of values). Therefore both IMPDH-Bs are inferior enzymes.

Identification of a major determinant of MPA resistance

MPA inhibits IMPDHs by an unusual mechanism [16]. The IMPDH reaction proceeds via the covalent intermediate E-XMP*, which forms when the active-site cysteine residue attacks the C2 position of IMP, transferring a hydride to NAD^+ [13]. The resulting NADH dissociates, allowing MPA to bind to E-XMP*, preventing hydrolysis to form XMP. The crystal structure of the E-XMP*–MPA complex has been solved for Chinese-hamster ovary IMPDH type 2 [17], revealing that MPA stacks against the purine ring of E-XMP* in a similar manner to the nicotinamide of NAD^+. Surprisingly, all of the residues within 4 Å (1 Å = 0.1 nm) of MPA are completely conserved in the fungal IMPDHs (Figure 5). Likewise, the IMP-binding site is also highly conserved. Only residue 411 is variable (Chinese-hamster ovary IMPDH2 numbering); the IMPDH-A enzymes contain a tyrosine residue at this site, whereas IMPDH-B enzymes have phenylalanine residues (Figure 5). Substitution of phenylalanine for Tyr^{411} did not increase the MPA resistance of *Pb*IMPDH-A, nor did the substitution of tyrosine for Phe^{411} decrease the MPA resistance of *Pb*IMPDH-B (Table 2). Therefore the structural determinants of MPA resistance must reside outside the active site.

Inspection of the structure suggested that the C-terminal segment (residues 498–527) was another likely candidate for a structural determinant of MPA resistance (Figure 5). This region includes part of the site that binds a monovalent cation activator, as well as segments that interact with the active site residues. Deletion of this segment inactivates the enzyme [18]. Swapping the 30-residue C-terminal segments revealed that this region is responsible for ~7 of the 60-fold difference in MPA resistance between *Pb*IMPDH-A and *Pb*IMPDH-B (see Table 2). Additional structural determinants of MPA resistance remain to be identified.

DISCUSSION

Phylogenetic analysis indicates that the IMPDH gene was duplicated before the radiation of *Penicillium* subgenus *Penicillium* (Figure 4 and see Supplementary Figure S4 at http://www.BiochemJ.org/bj/441/bj4410219add.htm). No remnants of the MPA biosynthetic cluster are present in *P. chrysogenum*, which suggests that the ability to produce MPA arrived after duplication of the IMPDH genes. Consistent with this hypothesis, both IMPDHs from the MPA-producer *P. brevicompactum* are more resistant to MPA than the IMPDHs from *A. nidulans* and *P. chrysogenum*. Thus both *P. brevicompactum* IMPDH-A and IMPDH-B have evolved in response to the presence of MPA. *Pb*IMPDH-B is 1000-fold more resistant than typical eukaryotic IMPDHs. The structural basis of these functional differences is not readily discernible. Whereas prokaryotic IMPDHs contain substitutions in their active sites that can account

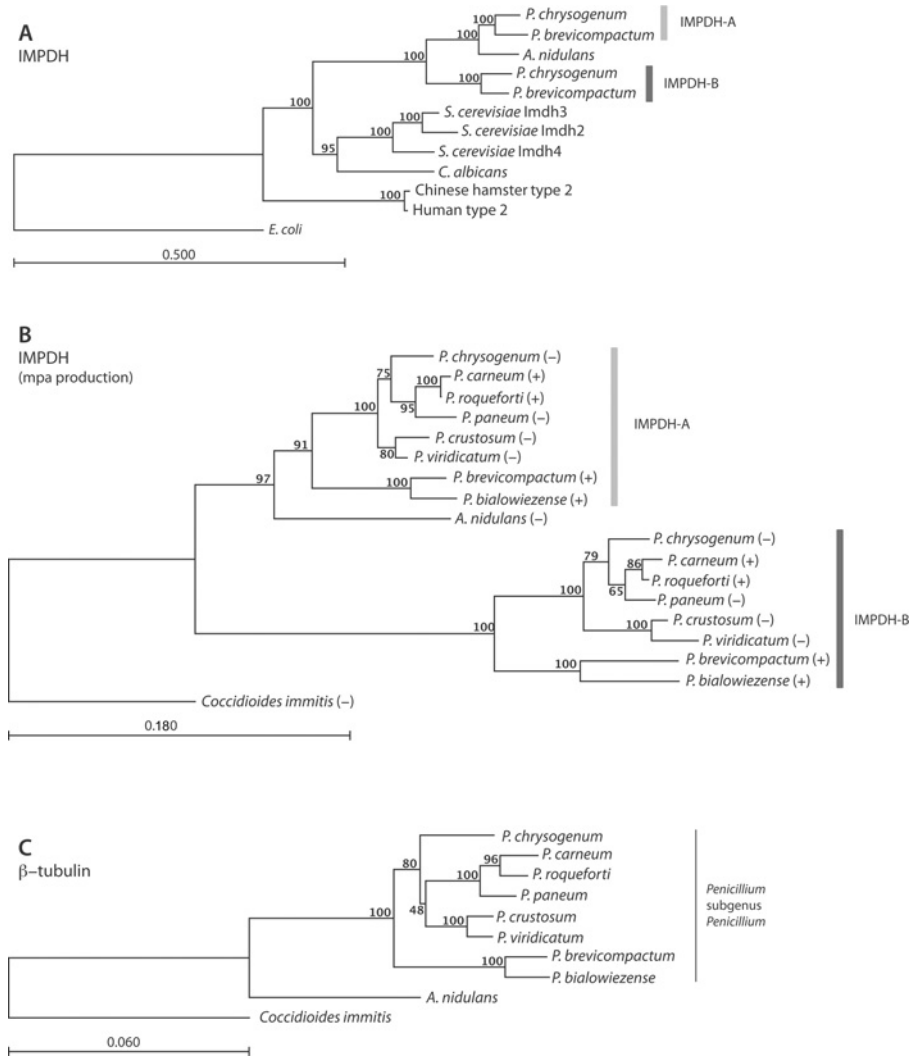

Figure 4 IMPDH phylogeny

(**A**) Rooted cladogram based on full-length amino acid sequences. (**B** and **C**) Rooted cladograms based on (**B**) IMPDH cDNA sequences (372–387 bp) and (**C**) β-tubulin cDNA sequences (950 bp) from eight species from *Penicillium* subgenus *Penicillium* and two filamentous fungi outside. *P.*, *Penicillium* and *A.*, *Aspergillus*. Bootstrap values (expressed as percentages of 1000 replications) are shown at the branch points, and the scale represents changes per unit. In (**B**), MPA production is indicated by + or −. The subclades with *Penicillium* subgenus *Penicillium* genes are marked in light grey (IMPDH-A) and dark grey (IMPDH-B). *E. coli* has been used as an outgroup in (**A**), and *C. immitis* as an outgroup in (**B**) and (**C**).

for MPA resistance, no such substitutions are present in the *P. brevicompactum* IMPDHs. The substitution of serine or threonine for Ala^{249} is associated with MPA resistance in *C. albicans* and *S. cerevisiae* [14,15]. This substitution is found in *Pb*IMPDH-A, but not in the more resistant *Pb*IMPDH-B. Substitutions at positions 277 and 462 have also resulted in modest MPA resistance [19], and substitutions at position 351 are proposed to cause resistance [20], but again no correlation is observed in the fungal IMPDHs. We identified the C-terminal segment as a new structural determinant of MPA sensitivity, but this segment accounts for only 7 of the 60-fold difference in resistance between *Pb*IMPDH-B and *Pb*IMPDH-B. Importantly, the extraordinary resistance of *Pb*IMPDH-B comes with a catalytic cost as this enzyme has lost much of the catalytic power of a typical IMPDH, with values of K_m (IMP) that are ~100-fold greater and k_{cat}/K_m (IMP) that are 100–1000-fold lower than 'normal'. This observation suggests that *Pb*IMPDH-B would be a very poor catalyst at normal cellular IMP concentrations of 20–50 μM [21]. However, IMP concentrations increase 10–35-fold in the presence of MPA [1,22,23]. Thus *P. brevicompactum* may contain millimolar concentrations of IMP during MPA biosynthesis, so that the turnover of *Pb*IMPDH-B would be comparable with a 'normal' fungal IMPDH.

Curiously, MPA production does not follow the phylogenetic relationship established by analysis of the IMPDH and β-tubulin genes (Figure 4). *P. chrysogenum* does not contain MPA-biosynthetic genes, although MPA producers are found on the neighbouring branches of the phylogenetic tree. As noted above, *P. chrysogenum* is more resistant to MPA than is *A. nidulans* (Figure 2A). This resistance could be the result of a gene-dosage effect as MPA resistance is associated with amplification of IMPDH genes in several organisms, consistent with this hypothesis [20,24–27]. We propose that the presence of two IMPDH genes in *Penicillium* subgenus *Penicillium* was permissive for MPA production. The failure to observe MPA production in other *Penicillium* species may reflect inappropriate culture conditions rather than absence of the biosynthetic cluster. If so, it is possible that MPA biosynthesis has been obtained in several independent events. It will be interesting to map the evolution of MPA biosynthesis and resistance as more genomic sequences of filamentous fungi become available.

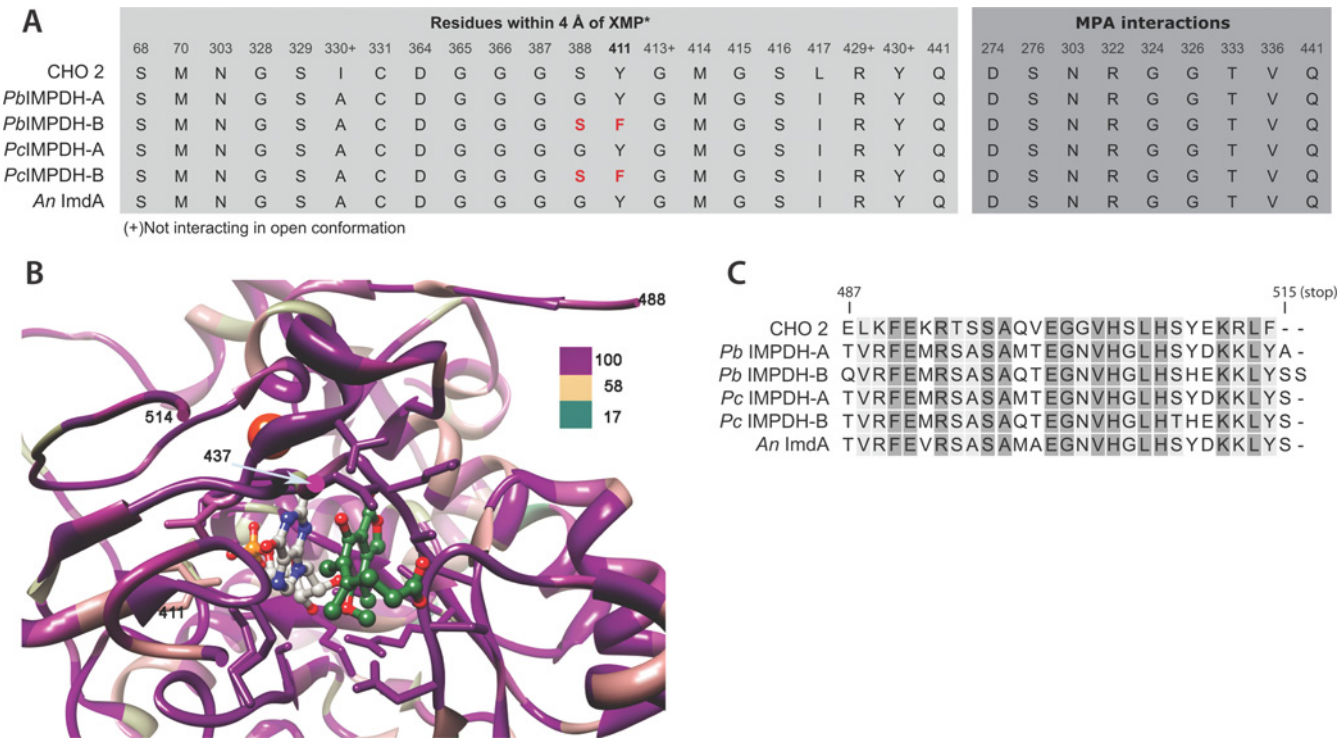

Figure 5 The MPA-binding site is conserved among drug-sensitive and drug-resistant eukaryotic IMPDHs

(**A**) Amino acid polymorphism in IMPDH of *A. nidulans* (*An*), *P. brevicompactum* (*Pb*) and *P. chrysogenum* (*Pc*). Shown are residues within 4 Å of E-XMP* (XMP*) and MPA. Residues in red are polymorphic between IMPDH-A and IMPDH-B. (**B**) An alignment of IMPDH-A and IMPDH-B from *P. brevicompactum* 23078 and *P. chrysogenum*, IMPDH-A from *A. nidulans* and IMPDH2 from Chinese-hamster ovary (CHO) was mapped on to the X-ray crystal structure of the MPA complex of Chinese-hamster ovary IMPDH (PDB code 1JR1) [17]. Key: 100 % conserved, dark magenta; 58 % conserved, tan; 17 % conserved, dark cyan. MPA, green ball and stick; IMP intermediate, grey ball and stick; K^+, gold; residues within 4 Å of MPA and IMP are shown in stick form. (**C**) Alignment of the C-terminal region. The region aligned represents the fragments that were swapped in the chimaeric *Pb*IMPDH-A and *Pb*IMPDH-B.

Table 2 MPA inhibition of fungal IMPDH variants

Phe^{411} is replaced with tyrosine in IMPDH-B and Tyr^{411} is replaced by phenylalanine in IMPDH-A*. nd, no data.

	IC_{50} (μM)			
Enzyme	Wild-type	411*	C-terminal swap	C-terminal swap + 411*
*Pb*IMPDH-A	0.43 ± 0.03	0.16 ± 0.02	3 ± 0.2	4.1 ± 0.3
*Pb*IMPDH-B	27 ± 9	25 ± 2	4.1 ± 0.3	3.1 ± 0.3
*An*ImdA	0.026 ± 0.002	0.026 ± 0.002	nd	nd

Gene duplication is generally believed to be a driving force in evolution, allowing one copy to diverge constraint-free, while the other copy maintains essential functions. The 'escape from adaptive conflict' subfunctionalization model is particularly attractive for the evolution of new enzyme activities [28,29]. In this model, duplication relieves the constraint of maintaining the original function and allows the emergence of enzymes with new catalytic properties. The blemish in this appealing hypothesis has long been recognized: most mutations are deleterious, so that the extra copy is quickly lost or converted into a pseudogene. Although several elegant and rigorous investigations of the *in vitro* evolution of new enzyme function demonstrate the feasibility of subfunctionalization (reviewed in [29,30]), genetic drift is widely recognized as the dominant mechanism in the wider evolution field. Several observations suggest that the emergence of MPA-resistant *Pb*IMPDH-B could be an example of neofunctionalization by a classic Ohno-type mechanism: a duplication followed by (largely deleterious) drift until a new environment, MPA production, provides a selection.

*Pc*IMPDH-B displays the effects of deleterious genetic drift: this protein is labile to proteolysis, and the value of k_{cat} ~1 % of that of typical eukaryotic IMPDH. Microarray data indicate that *P. chrysogenum* expresses both IMPDH-A and IMPDH-B under most conditions, so at present there is no evidence for specialized functions for these genes [31,32]. We cannot rule out the possibility that *Pc*IMPDH-B plays another role within the cell, perhaps by interacting with another protein, or even as a heterotetramer with *Pc*IMPDH-A. Nevertheless, our data suggest that the enzymatic properties of both IMPDH-Bs have declined over the course of evolution. In the case of *P. brevicompactum*, gaining the ability to produce MPA may have rescued IMPDH-B from non-functionalization.

AUTHOR CONTRIBUTION

Bjarne Hansen, Hans Genee, Xin Sun and Lizbeth Hedstrom wrote the paper. All authors contributed to the editing of the paper before submission. Bjarne Hansen, Hans Genee, Christian Kaas and Jakob Nielsen built constructs and performed degenerate PCR and spot assays. Bjarne Hansen and Hans Genee performed the bioinformatics analysis. Xin Sun purified the proteins, performed the biochemical analysis and carried out the complementation experiment. Uffe Mortensen, Jens Frisvad and Lizbeth Hedstrom contributed to experimental design. Lizbeth Hedstrom supervised the project.

ACKNOWLEDGEMENT

We thank Martin Engelhard Kornholt for valuable technical assistance in the laboratory.

FUNDING

This work was supported by The Danish Council for Independent Research Technology and Production Sciences [grant numbers 09-064967 and 09-064240 (to B.G.H. and U.H.M.)] and by the National Institutes of Health [grant number GM054403 (to L.H.)].

REFERENCES

1 Bentley, R. (2000) Mycophenolic acid: a one hundred year odyssey from antibiotic to immunosuppressant. Chem. Rev. **100**, 3801–3826
2 Regueira, T. B., Kildegaard, K. R., Hansen, B. G., Mortensen, U. H., Hertweck, C. and Nielsen, J. (2011) Molecular basis for mycophenolic acid biosynthesis in *Penicillium brevicompactum*. Appl. Environ. Microbiol. **77**, 3035–3043
3 Hansen, B. G., Genee, H. J., Kaas, C. S., Nielsen, J. B., Mortensen, U. H., Frisvad, J. C. and Patil, K. R. (2011) A new clade of IMP dehydrogenases with a role in self-resistance in mycophenolic acid producing fungi. BMC Microbiol. **11**, 202
4 Frisvad, J. C. and Samson, R. A. (2004) Polyphasic taxonomy of *Penicillium* subgenus *Penicillium*: a guide to identification of food and air-borne terverticillate Penicillia and their mycotoxins. Stud. Mycol. **49**, 1–174
5 Geu-Flores, F., Nour-Eldin, H. H., Nielsen, M. T. and Halkier, B. A. (2007) USER fusion: a rapid and efficient method for simultaneous fusion and cloning of multiple PCR products. Nucleic Acids Res. **35**, e55
6 Hansen, B. G., Salomonsen, B., Nielsen, M. T., Nielsen, J. B., Hansen, N. B., Nielsen, K. F., Regueira, T. B., Nielsen, J., Patil, K. R. and Mortensen, U. H. (2011) Versatile enzyme expression and characterization system for *Aspergillus nidulans*, with the *Penicillium brevicompactum* polyketide synthase gene from the mycophenolic acid gene cluster as a test case. Appl. Environ. Microbiol. **77**, 3044–3051
7 Norholm, M. H. (2010) A mutant Pfu DNA polymerase designed for advanced uracil-excision DNA engineering. BMC Biotechnol. **10**, 21
8 MacPherson, I. S., Kirubakaran, S., Gorla, S. K., Riera, T. V., D'Aquino, J. A., Zhang, M., Cuny, G. D. and Hedstrom, L. (2010) The structural basis of *Cryptosporidium*-specific IMP dehydrogenase inhibitor selectivity. J. Am. Chem. Soc. **132**, 1230–1231
9 Wang, W., Papov, V. V., Minakawa, N., Matsuda, A., Biemann, K. and Hedstrom, L. (1996) Inactivation of inosine 5′-monophosphate dehydrogenase by the antiviral agent 5-ethynyl-1-β-D-ribofuranosylimidazole-4-carboxamide 5′-monophosphate. Biochemistry **35**, 95–101
10 Frisvad, J. C., Smedsgaard, J., Larsen, T. O. and Samson, R. A. (2004) Mycotoxins, drugs and other extrolites produced by species in *Penicillium* subgenus *Penicillium*. Stud. Mycol. **49**, 201–241
11 Chooi, Y. H., Cacho, R. and Tang, Y. (2010) Identification of the viridicatumtoxin and griseofulvin gene clusters from *Penicillium aethiopicum*. Chem. Biol. **17**, 483–494
12 Gao, X., Chooi, Y. H., Ames, B. D., Wang, P., Walsh, C. T. and Tang, Y. (2011) Fungal indole alkaloid biosynthesis: genetic and biochemical investigation of the tryptoquialanine pathway in *Penicillium aethiopicum*. J. Am. Chem. Soc. **133**, 2729–2741
13 Hedstrom, L. (2009) IMP dehydrogenase: structure, mechanism and inhibition. Chem. Rev. **109**, 2903–2928
14 Kohler, G. A., Gong, X., Bentink, S., Theiss, S., Pagani, G. M., Agabian, N. and Hedstrom, L. (2005) The functional basis of mycophenolic acid resistance in *Candida albicans* IMP dehydrogenase. J. Biol. Chem. **280**, 11295–11302
15 Jenks, M. H. and Reines, D. (2005) Dissection of the molecular basis of mycophenolate resistance in *Saccharomyces cerevisiae*. Yeast **22**, 1181–1190
16 Link, J. O. and Straub, K. (1996) Trapping of an IMP dehydrogenase-substrate covalent interemediate by mycophenolic acid. J. Am. Chem. Soc. **118**, 2091–2092
17 Sintchak, M. D., Fleming, M. A., Futer, O., Raybuck, S. A., Chambers, S. P., Caron, P. R., Murcko, M. and Wilson, K. P. (1996) Structure and mechanism of inosine monophosphate dehydrogenase in complex with the immunosuppressant mycophenolic acid. Cell **85**, 921–930
18 Nimmesgern, E., Black, J., Futer, O., Fulghum, J. R., Chambers, S. P., Brummel, C. L., Raybuck, S. A. and Sintchak, M. D. (1999) Biochemical analysis of the modular enzyme inosine monophosphate dehydrogenase. Protein Expression Purif. **17**, 282–289
19 Farazi, T., Leichman, J., Harris, T., Cahoon, M. and Hedstrom, L. (1997) Isolation and characterization of mycophenolic acid resistant mutants of inosine 5′-monophosphate dehydrogenase. J. Biol. Chem. **272**, 961–965
20 Lightfoot, T. and Snyder, F. F. (1994) Gene amplification and dual point mutations of mouse IMP dehydrogenase associated with cellular resistance to mycophenolic acid. Biochim. Biophys. Acta **1217**, 156–162
21 Hartman, N., Ahluwalia, G., Cooney, D., Mitsuya, H., Kageyama, S., Fridland, A., Broder, S. and Johns, D. (1991) Inhibitors of IMP dehydrogenase stimulate the phosphorylation of the anti-human immunodeficiency virus nucleosides 2′,3′-dideoxyadenosine and 2′,3′-dideoxyinosine. Mol. Pharm. **40**, 118–124
22 Balzarini, J., Karlsson, A., Wang, L., Bohman, C., Horská, K., Votruba, I., Fridland, A., Van Aerschot, A., Hedewijn, P. and De Clerq, E. (1993) EICAR (5-ethynyl-1-β-D-ribofuranosylimidazole-4-carboxamide): a novel potent inhibitor of inosinate dehydrogenase activity and guanylate biosynthesis. J. Biol. Chem. **33**, 24591–24598
23 Wu, J. C. (1994) Mycophenolate mofetil: molecular mechanisms of action. Perspect. Drug Discovery Des. **2**, 185–204
24 Collart, F. R. and Huberman, E. (1987) Amplification of the IMP dehydrogenase gene in Chinese hamster cells reistant to mycophenolic acid. Mol. Cell. Biol. **7**, 3328–3331
25 Wilson, K., Collart, F., Huberman, E., Stringer, J. and Ullman, B. (1991) Amplification and molecular cloning of the IMP dehydrogenase gene of *Leishmania donovani*. J. Biol. Chem. **266**, 1665–1671
26 Wilson, K., Berens, R. L., Sifri, C. D. and Ullman, B. (1994) Amplification of the inosinate dehydrogenase gene in *Trypanosoma brucei gambienese* due to an increase in chromosome copy number. J. Biol. Chem. **269**, 28979–28987
27 Kohler, G. A., White, T. C. and Agabian, N. (1997) Overexpression of a cloned IMP dehydrogenase gene of *Candida albicans* confers resistance to the specific inhibitor mycophenolic acid. J. Bacteriol. **179**, 2331–2338
28 O'Brien, P. J. and Herschlag, D. (1999) Catalytic promiscuity and the evolution of new enzymatic activities. Chem. Biol. **6**, R91–R105
29 Khersonsky, O. and Tawfik, D. S. (2010) Enzyme promiscuity: a mechanistic and evolutionary perspective. Annu. Rev. Biochem. **79**, 471–505
30 Tracewell, C. A. and Arnold, F. H. (2009) Directed enzyme evolution: climbing fitness peaks one amino acid at a time. Curr. Opin. Chem. Biol. **13**, 3–9
31 van den Berg, M. A., Albang, R., Albermann, K., Badger, J. H., Daran, J. M., Driessen, A. J., Garcia-Estrada, C., Fedorova, N. D., Harris, D. M., Heijne, W. H. et al. (2008) Genome sequencing and analysis of the filamentous fungus *Penicillium chrysogenum*. Nat. Biotechnol. **26**, 1161–1168
32 Hoff, B., Kamerewerd, J., Sigl, C., Zadra, I. and Kück, U. (2010) Homologous recombination in the antibiotic producer *Penicillium chrysogenum*: strain ΔPcku70 shows up-regulation of genes from the HOG pathway. Appl. Microbiol. Biotechnol. **85**, 1081–1094
33 Saitou, N. and Nei, M. (1987) The neighbour-joining method: a new method for reconstructing phylogenetic trees. Mol. Biol. Evol. **4**, 406–425

Received 15 July 2011/31 August 2011; accepted 15 September 2011
Published as BJ Immediate Publication 15 September 2011, doi:10.1042/BJ20111278

Biochem. J. (2012) **441**, 219–226 (Printed in Great Britain) doi:10.1042/BJ20111278

online data

SUPPLEMENTARY ONLINE DATA

Adaptive evolution of drug targets in producer and non-producer organisms

Bjarne G. HANSEN*[1], Xin E. SUN†[2], Hans J. GENEE*, Christian S. KAAS*, Jakob B. NIELSEN*, Uffe H. MORTENSEN*, Jens C. FRISVAD* and Lizbeth HEDSTROM‡[3]

*Technical University of Denmark, Department of Systems Biology, Center for Microbial Biotechnology, 2800 Kgs Lyngby, Denmark, †Graduate Program in Biochemistry, Brandeis University, 415 South Street, Waltham, MA 02454, U.S.A., and ‡Departments of Biology and Chemistry, Brandeis University, 415 South Street, Waltham, MA 02454, U.S.A.

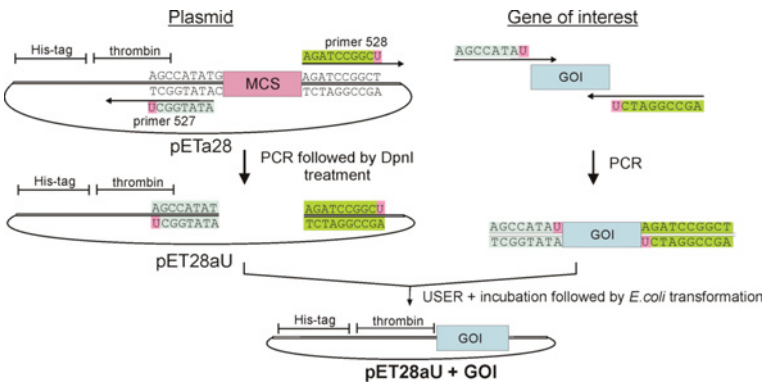

Figure S1 Detailed graphical representation showing the principle of PCR-based USER cloning of a GOI (gene of interest) into pET28a

A pET28a USER-compatible vector fragment, pET28aU, is made by PCR amplification using uracil-containing primers (527 and 528) followed by DpnI treatment to remove the PCR template. Likewise, the GOI fragment to be inserted into pET28aU is amplified with primers containing uracil. The primer tails were designed to allow seamless USER fusion; the uracil in the 5′-end of the GOI fragment corresponds to the T of the start codon (ATG) of the GOI, and the uracil in the 3′-end of the GOI fragment is complementary to the second nucleotide in the stop codon (TAG) of pET28a. USER fusion of the GOI PCR fragment and pET28aU is performed by mixing the two fragments, followed by USER enzyme treatment to remove uracil residues. This step generates ends with single-stranded DNA overhangs that allow for orderly fusion of the fragments. Following USER treatment, the cloning mixture is transformed into *E. coli*.

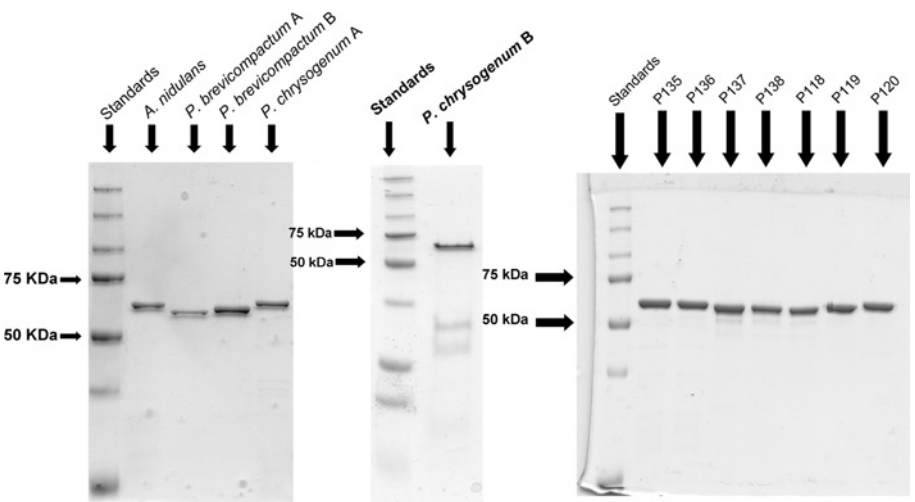

Figure S2 SDS/PAGE of purified recombinant fungal proteins

Lanes contents are as marked. All enzymes were purified to >90 % purity, with the exception of *Pc*IMPDH-B, which was only partially purified to ∼45 % purity because of poor stability. Note that the lower-molecular-mass bands in the *Pc*IMPDH-B sample are also IMPDH, as demonstrated by Western blot analysis. The concentrations of all enzymes were verified by titration with MPA as described in the main paper. This proteolysis could not be prevented with the addition of protease inhibitor cocktails to the lysate. P135, *Pb*IMPDH-B with *Pb*IMPDH-A C-terminus; P136, *Pb*IMPDH-B with *Pb*IMPDH-A C-terminus + F411Y mutation; P137, *Pb*IMPDH-A with *Pb*IMPDH-B C-terminus; P138, *Pb*IMPDH-A with *Pb*IMPDH-B C-terminus + Y411F mutation; P118, *Pb* IMPDH-A with Y411F mutation; P119, *Pb*IMPH-B with F411Y mutation; P120, *An*ImdA with Y411F mutation. Molecular masses are indicated in kDa.

[1] Present address: Novozymes A/S, Krogshoejvej 36, 2880 Bagsvaerd, Denmark.
[2] Present address: Department of Chemistry, Boston University, 590 Commonwealth Avenue, Boston, MA 02215-252, U.S.A.
[3] To whom correspondence should be addressed (email hedstrom@brandeis.edu).

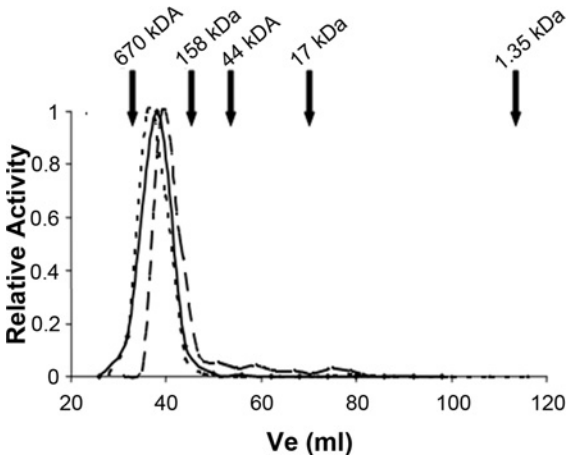

Figure S3 Determination of IMPDH oligomeric state using gel filtration chromatography on a S200 Sephacryl column

*An*ImdA (dotted line) elutes at 39.3 ml, *Pb*IMPDH-A (continuous line) elutes at 39.2 ml, and *Pb*IMPDH-B (dashed line) elutes at 39.0 ml. All three proteins elute at ~220 kDa, consistent with their being tetramers. The elution volumes (Ve) of the standards are as follows: Blue Dextran, 36 ml; thyroglobulin, 670 kDa, 36.2 ml; bovine γ-globulin, 158 kDa, 44 ml; chicken ovalbumin, 44 kDa, 56.9 ml; equine myoglobin, 17 kDa, 71.8 ml; vitamin B_{12}, 1.35 kDa, 117 ml.

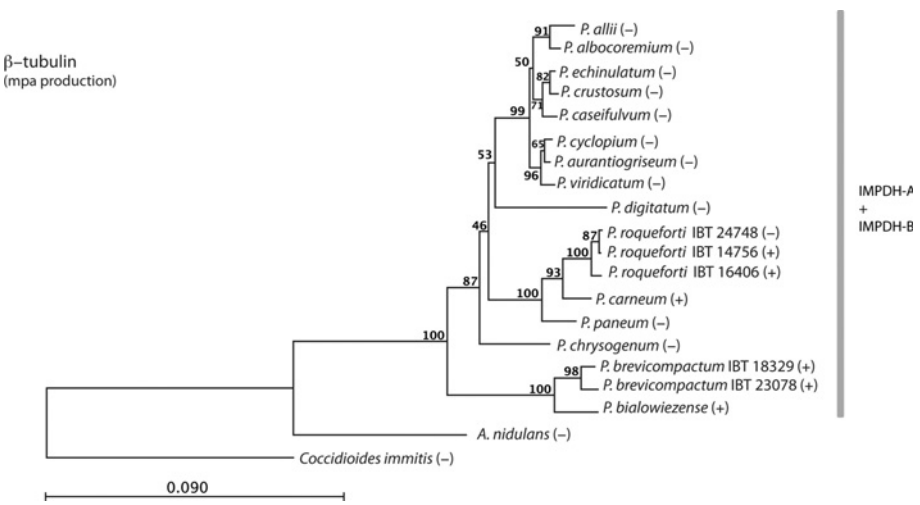

Figure S4 Rooted cladogram based on β-tubulin cDNA sequences (950 bp) from 14 species from *Penicillium* subgenus *Penicillium* and two other filamentous fungi

P., *Penicillium*; *A.*, *Aspergillus*. MPA production is indicated by $+$ or $-$. The grey line indicates organisms where both IMPDH-A and IMPDH-B genes have been detected. Bootstrap values (expressed as percentages of 1000 replications) are shown at the branch points, and the scale represents changes per unit. *Coccidioides immitis* has been used as an outgroup.

Table S1 Sequences generated in the present study

Species	IBT number	Other collection numbers	MPA production*	DNA sequences (GenBank® accession number)		
				IMPDH-A	IMPDH-B	β-Tubulin
P. allii	20212	CBS 875.95	−	JN112053	JN112066	JN112035
P. albocoremium†	21596	−	−	JN112054	JN112065	JN112036
P. aurantiogriseum†	11325	CBS 792.95	−	JN112050	JN112062	JN112033
P. brevicompactum†	18329	CBS 110067	++	JN112046	JN112068	JN112040
P. caseifulvum	19782	CBS 108956	−	JN112051	JN112067	JN112037
P. crustosum	21518	CBS 101025	−	JN112048	JN112061	JN112030
P. cyclopium†	16769	CBS 110337	−	JN112049	JN112063	JN112034
P. echinulatum†	21839	CBS 112286	−	JN112052	JN112064	JN112032
P. roqueforti	14756	−	+	JN112045	JN112058	JN112039
P. roqueforti†	24748	−	−	JN112044	JN112059	JN112038
P. viridicatum	21551	CBS 101034	−	JN112047	JN112060	JN112031

*MPA production on CYA medium: −, no production; +, medium production; ++, high production [1].

†The extracted *imdA* and *imdB* sequence parts for these organisms do not overlap and are therefore not included in Figure 5(B) of the main text.

Table S2 PCR primers

Underlined sequence will be removed and lead to a single-stranded overhang during USER cloning.

Primer	Sequence (5′→3′)
BGHA358	AGGCCAGCUCGTGAAAGCCTTCCGTGGTATG
BGHA359	AGCTGGCCUTCGTTGCTGACAAAGTACTC
BGHA360	AGGTCAGCUGGTCAAGGCCTACCGCGGTATG
BGHA361	AGCTGACCUTCATTGCTAACGTAGTACTC
BGHA430	AAGCCGATGUAACCGGGCAGGATCAGGA
BGHA431	ACATCGGCTUCCCCGCTTCCGATGTCTCATTG
BGHA432	AGGGTTCCGTTCUCAGTGACAGGGAAGCCACCGAAG
BGHA433	AGAACGGAACCCUTAAGTCCAAGCTCGTTGGA
BGHA434	AAGGTGAUAGAACCGGGCAAAATCAGGA
BGHA435	ATCACCTUCCCGGCATCGGATGTTTCGT
BGHA436	AGGGTTCCCTTTUCGGTCACCGGGAACCCGCCGA
BGHA437	AAAAGGGAACCCUCCTCTCGAAGCTTCTCGGA
BGHA454	ACGGAAGGCCUTGACGAGCTGGCCCTCGTTG
BGHA455	ATTGGGGTGGCCTCUCTCATGAGCACTGAAGTTCTTTC
BGHA505	AGCCGATGUAGCCGGGCAAGATCAGGA
BGHA506	ACATCGGCUTCCCTGCCTCCGATGTGT
BGHA507	AGTTCCGTUCTCAGTGACAGGGAAACCTCC
BGHA508	AACGGAACUCTTCGCTCCAAGCTCGTT
BGHA509	AACCGATAUATCCCGGAAGAATGAGGAA
BGHA510	ATATCGGTUTTCCTGCTTCCGATGTTAC
BGHA511	ATTTTCAGUAACTGGGAAGCCGCCGAA
BGHA512	ACTGAAAAUGGAACTCTCCGCTCAAAG
BGHA527	ATATGGCUGCCGCGCGGCACC
BGHA528	AGATCCGGCUGCTAACAA
BGHA529	AGCCATAUGGTCGAAATCCTGGACTA
BGHA530	AGCCGGATCUAAGAAGAGTACAACTTCTTCTCG
BGHA539	AGCCATAUGCCTATCACCGCCAGCGAC
BGHA540	AGCCGGATCUACGCGTAAAGCTTCTTGTCG
BGHA541	AGCCATAUGGTCGAAGTTCTGGATTATAC
BGHA542	AGCCGGATCUAAGAGTACAACTTCTTCTC
BGHA543	AGCCATAUGCCTATCACCGCCGGCGAC
BGHA544	AGCCGGATCUACGAGTAAAGCTTCTTGTC
BGHA545	AGCCATAUGCCAATTGCCAACGGTGAC
BGHA546	AGCCGGATCUAAGAGTAGAGCTTCTTGTC
BGHA667	ACGGTTCCGUTGTTCACACCGGTGTGCA
BGHA668	ACGGAACCGUTCGCTTTGAAATGCGCAG
BGHA669	ACCTGGCCGUTGTCGACACCAGCGTGCA
BGHA670	ACGGCCAGGUTCGCTTTGAGATGAGAAG
BGHA236HC	ATGCCIATYNCCRMCGGIGAYKC
BGHA246HC	CRGCCTTCTTRTCCTCCATGG
BGHA531	AGCTTCTTGTCGTAGCTGTG
BGHA532	GTCAAGGGTCTSGCYATGG
BGHA240HC	ATGGTCGADRTYCWGGAYTAYACC
BGHA241HC	GARGCRCCRGCGTTMTTG
BGHA343	GAGCGYATGARYGTYTAYTTCA
BGHA344	GTGAACTCCATCTCRTCCATACC

Table S3 *E. coli* expression constructs and cloning strategy

Construct	Enzyme expressed	Primers for IMPDH amplification		
		Exon 1	Exon 2	Exon 3
P113	*Pb*IMPDH-A	BGHA539/BGHA505	BGHA506/BGHA507	BGHA508/BGHA540
P114	*Pb*IMPDH-B	Amplified from cDNA with BGHA529/BGHA530		
P115	*A. nidulans* ImdA	BGHA545/BGHA509	BGHA510/BGHA511	BGHA512/BGHA546
P116	*Pc*IMPDH-A	BGHA543/BGHA430	BGHA431/BGHA432	BGHA433/BGHA544
P117	*Pc*IMPDH-B	BGHA541/BGHA434	BGHA435/BGHA436	BGHA437/BGHA542
P118	*Pb*IMPDH-A with Y411F mutation	BGHA539/BGHA455 and BGHA540/BGHA454 and P113 as PCR template		
P119	*Pb*IMPDH-B with F411Y mutation	BGHA529/BGHA361 and BGHA530/BGHA360 and P114 as PCR template		
P120	*An*ImdA with Y411F mutation	BGHA545/BGHA359 and BGHA546/BGHA358 and P115 as PCR template		
P135	Chimaeric IMPDH of *Pb*IMPDH-B (N-terminus) and *Pb*IMPDH-A C-terminus	*Pb*IMPDH-B and *Pb*IMPDH-A fragments amplified with primer pairs BGHA529/BGHA667 and BGHA668/BGHA540 respectively		
P136	*Pb*IMPDH-B with F411Y mutation and *Pb*IMPDH-A C-terminus	Same as for P135, but using P119 as PCR template for IMPDH-B fragment		
P137	Chimaeric IMPDH of *Pb*IMPDH-A (N-terminus) and *Pb*IMPDH-B C-terminus	*Pb*IMPDH-A and *Pb*IMPDH-B fragments amplified with primer pairs BGHA539/BGHA669 and BGHA670/BGHA530 respectively		
P138	*Pb*IMPDH-A with Y411F mutation and with *Pb*IMPDH-B C-terminus	Same as for P137, but using P118 as PCR template for IMPDH-A fragment		

Table S4 Concentrations of IMP and NAD^+ used for determination of IC_{50} (MPA)

Enzyme	IMP (mM)	NAD^+ (mM)
*An*ImdA	0.5	0.5
*Pb*IMPDH-A	3	1
*Pb*IMPDH-B	3	1
*Pc*IMPDH-A	1	1
*Pc*IMPDH-B	1	1
Mutant proteins	1	1

Table S5 Putative genes flanking the MPA cluster in *P. brevicompactum*

Further comparison of the regions further away from the MPA cluster in *P. brevicompactum* reveal other genes homologous with genes from *P. chrysogenum*; however, they are located in loci of many different contigs.

Gene	Region on *P. brevicompactum* contig (*Pb* BAC 1E13 + 1C23)*	Size (number of amino acids)	BLASTx homologue	Predicted function	E-value	Identity (%)
orf1	0–4139	987	*P. chrysogenum*, Pc22g22260	C2H2 finger domain protein	0	87
orf2	4513–5736	407	*P. chrysogenum*, Pc22g22270	DNA mismatch repair protein	1.15×10^{-151}	76
orf3	7554–9212	514	*P. chrysogenum*, Pc22g22280	WD repeat protein	0	94
orf4	10249–10913	191	*P. chrysogenum*, Pc22g22290	IgE-binding protein	5.97×10^{-75}	82
orf5	12809–1399	360	*Neosartorya fischeri*, XP_001265454	Nucleoside diphosphatase	1.42×10^{-113}	71
			P. chrysogenum, Pc22g22320	Nucleoside diphosphatase	1.37×10^{-93}	72
MPA cluster (17830– 43315)						
orf13	50594–51894	368	*P. chrysogenum*, Pc21g04710	Phospho-2-dehydro-3-deoxyheptonate aldolase	0	94
orf14	52993–53878	256	*P. chrysogenum*, Pc21g04720	Unknown	4.00×10^{-91}	72
orf15	54299–55162	251	*P. chrysogenum*, Pc21g04730	Unknown	1.61×10^{-63}	60
orf16	55381–56121	246	*Aspergillus fumigatus*, XP_001481519 (no hits in *P. chrysogenum*)	Glycosidase hydrolase	1.00×10^{-61}	57
orf17	57170–59032	597	*P. chrysogenum*, Pc21g04750	C6 transcription factor	0	81
orf18	60261–62432	539	*P. chrysogenum*, Pc21g04770	NADH-cytochrome B5 reductase	6.63×10^{-115}	76
orf19	63597–65642	625	*P. chrysogenum*, Pc21g04800	Unknown	0	73
orf20	67638–68559	286	*P. chrysogenum*, Pc12g02580	Unknown	3.54×10^{-44}	62
orf21	68851–72867	1255	*P. chrysogenum*, Pc12g02550	Myosin protein	0	93
orf22	74083–79557	1181	*P. chrysogenum*, Pc22g21120	Carboxypeptidase	0	79
orf23	79786–82071	689	*P. chrysogenum*, Pc12g02500	Arginine permease	0	85
orf24	84043–85074	293	*Aspergillus niger*, XP_001391260 (no hits in *P. chrysogenum*)	Phytanoyl-CoA dioxygenase	3.30×10^{-130}	74
orf25	85889–91912	1907	*Aspergillus terreus*, XP_001209574	Unknown	0	37
			P. chrysogenum, Pc21g03870	Unknown	9.85×10^{-142}	27
orf26	93143–100908	2119	*Penicillium marneffei*, XP_002147174	β-Galactosidase	0	74
			P. chrysogenum, Pc22g14540	β-Galactosidase	0	38
orf27	101641–103365	574	*P. chrysogenum*, Pc21g21450	Unknown	0	61

REFERENCE

1 Frisvad, J. C. and Samson, R. A. (2004) Polyphasic taxonomy of *Penicillium* subgenus *Penicillium*: a guide to identification of food and air-borne terverticillate Penicillia and their mycotoxins. Stud. Mycol. **49**, 1–174

Received 15 July 2011/31 August 2011; accepted 15 September 2011
Published as BJ Immediate Publication 15 September 2011, doi:10.1042/BJ20111278